Research Paper

S-allyl cysteine reduces osteoarthritis pathology in the tert-butyl hydroperoxide-treated chondrocytes and the destabilization of the medial meniscus model mice via the Nrf2 signaling pathway

Zhenxuan Shao[1,2,3], Zongyou Pan[4], Jialiang Lin[1,2,3], Qingqian Zhao[3], Yuqian Wang[3], Libin Ni[1,2,3], Shiyi Feng[1,2,3], Naifeng Tian[1,2,3], Yaosen Wu[1,2,3], Liaojun Sun[1,2,3], Weiyang Gao[1,2,3], Yifei Zhou[1,2,3], Xiaolei Zhang[1,2,3,5], Xiangyang Wang[1,2,3]

[1]Department of Orthopaedics, The Second Affiliated Hospital and Yuying Children's Hospital of Wenzhou Medical University, Wenzhou, Zhejiang Province, China
[2]Key Laboratory of Orthopedics of Zhejiang Province, Wenzhou, Zhejiang Province, China
[3]The Second School of Medicine, Wenzhou Medical University, Wenzhou, Zhejiang Province, China
[4]Department of Orthopedics, The Second Affiliated Hospital, School of Medicine, Zhejiang University, Hangzhou, Zhejiang Province, China
[5]Chinese Orthopedic Regenerative Medicine Society, Hangzhou, Zhejiang Province, China

Correspondence to: Xiangyang Wang, Xiaolei Zhang, Yifei Zhou; **email:** xiangyangwang@wmu.edu.cn, zhangxiaolei@wmu.edu.cn, yifeizhou@wmu.edu.cn
Keywords: S-allyl cysteine, osteoarthritis, senescence, apoptosis, extracellular matrix
Received: February 28, 2020 **Accepted:** June 19, 2020 **Published:** October 7, 2020

ABSTRACT

In this study, we used murine chondrocytes as an *in vitro* model and mice exhibiting destabilization of the medial meniscus (DMM) as an *in vivo* model to investigate the mechanisms through which S-allyl cysteine (SAC) alleviates osteoarthritis (OA). SAC significantly reduced apoptosis and senescence and maintained homeostasis of extracellular matrix (ECM) metabolism in tert-butyl hydroperoxide (TBHP)-treated chondrocytes. Molecular docking analysis showed a –CDOCKER interaction energy value of 203.76 kcal/mol for interactions between SAC and nuclear factor erythroid 2-related factor 2 (Nrf2). SAC increased the nuclear translocation of Nrf2 and activated the Nrf2/HO1 signaling pathway in TBHP-treated chondrocytes. Furthermore, Nrf2 knockdown abrogated the antiapoptotic, antisenescence, and ECM regulatory effects of SAC in TBHP-treated chondrocytes. SAC treatment also significantly reduced cartilage ossification and erosion, joint-space narrowing, synovial thickening and hypercellularity in DMM model mice. Collectively, these findings show that SAC ameliorates OA pathology in TBHP-treated chondrocytes and DMM model mice by activating the Nrf2/HO1 signaling pathway.

INTRODUCTION

Osteoarthritis (OA) is a progressive and degenerative joint disease that causes severe joint pain, limits daily activities, and eventually leads to disability [1]. OA affects nearly 27 million patients in the United States and over 250 million individuals worldwide [2, 3]. The current treatments for OA are limited to symptomatic pain relief and nonsteroidal anti-inflammatory drugs (NSAIDs) in the early stages and joint replacement surgery in the advanced stages [2]. Advanced treatments such as cartilage tissue engineering [4] and stem cell therapy [5] have not shown promising results for OA. Hence, there is an urgent need to develop novel effective therapies for OA.

Reactive oxygen species (ROS) play a crucial role in OA pathology [6–8]. ROS-related proteins are differentially

expressed in both human and mouse OA cartilage tissues [9, 10]. Furthermore, OA-related factors, such as mechanical loading [9], aging [11] and inflammation [12, 13] cause mitochondrial dysfunction, which promotes excessive ROS production [14, 15]. High and sustained ROS accumulation promotes senescence [16, 17], apoptosis [18, 19], and imbalanced extracellular matrix (ECM) turnover [20, 21] of the chondrocytes. This suggests that ROS regulation is important for OA treatment.

OA affects all the tissues in the articular joints, but the hallmark feature of OA is the structural destruction and dysfunction of the cartilage tissue [22]. The chondrocytes regulate extracellular matrix (ECM) synthesis and homeostasis of the cartilage tissue [23]. OA-related chondrocytes demonstrate excessive senescence [24, 25] and apoptosis [26, 27] compared to the normal chondrocytes. Moreover, OA cartilage shows increased breakdown (catabolism) and decreased synthesis (anabolism) of the ECM [28]. Furthermore, targeting senescence, apoptosis and ECM metabolism has shown promising trends for OA therapy [29].

Previous studies have shown that a vegetable-rich diet, especially including garlic, protects against OA progression [30, 31]. The major biologically active compound in garlic is S-allyl cysteine (SAC), which protects against neurodegeneration, kidney injury, and inflammation [32–35]. However, the therapeutic effects of SAC on OA progression have not been investigated.

In the current study, we induced excessive ROS in murine chondrocytes using tert-butyl hydroperoxide or TBHP [36–38], and investigated the protective effects of SAC. We also performed bioinformatics analysis using molecular docking algorithm and functional experiments to identify the underlying mechanisms of SAC. We also studied the *in vivo* effects of SAC on OA using the destabilization of the medial meniscus (DMM) mouse model.

RESULTS

SAC maintains the viability of TBHP-treated chondrocytes in a dose-dependent manner

The chemical structure of SAC is shown in Figure 1A. We performed the CCK-8 assay to determine the viability of chondrocytes treated with ascending concentrations of SAC (0, 12.5, 25, 50, 100, 200μM) for 24 h. The viability of chondrocytes treated with SAC concentrations below 100μM was comparable to controls, but, 200μM SAC reduced chondrocyte viability (Figure 1B). Therefore, we chose SAC concentrations below 100μM for further experiments.

Next, we analyzed the cytoprotective effects of SAC on TBHP-treated chondrocytes using the CCK-8 assay. TBHP significantly reduced the viability of chondrocytes (Supplementary Figure 2), but SAC reduced the cytotoxic effects of THBP in a dose dependent manner, with 100μM SAC showing maximal effects (Figure 1C). Furthermore, microscopic observation showed that TBHP-treated chondrocytes had shrunk in size and were floating in the medium, whereas SAC-treated chondrocytes maintained their normal size, morphology, and adherence properties (Figure 1D). These results show that SAC maintains the viability of TBHP-treated chondrocytes in a dose dependent manner.

SAC maintains extracellular matrix homeostasis in TBHP-treated chondrocytes

We then analyzed Aggrecan and collagen II (COL2) expression to determine ECM biosynthesis (anabolism) and the expression of ADAM metallopeptidase with thrombospondin type 1 motif 5 (ADAMTS5), matrix metallopeptidase 3 (MMP3), and matrix metallopeptidase 3 (MMP13) to determine ECM breakdown (catabolism). Western blotting and immunofluorescence analyses showed that THBP treatment significantly reduced the expression of Aggrecan (Figure 2A, 2B) and COL2 (Figure 2C, 2D), whereas SAC treatment restored ECM biosynthesis in a dose-dependent manner (Figure 2A–2D). Moreover, TBHP treatment significantly increased ADAMTS5, MMP3 and MMP13 expression, thereby indicating enhanced ECM breakdown, but, SAC reduced ECM breakdown induced by TBHP in a dose-dependent manner (Figure 2A, 2B). These results show that SAC treatment protects chondrocytes against dysregulation of ECM metabolic homeostasis by TBHP in a dose dependent manner.

SAC protects TBHP-treated chondrocytes against senescence

Next, we analyzed if SAC protects chondrocytes against senescence using senescence-associated β-galactosidase (SA-β-gal) staining and 5-ethynyl-2'-deoxyuridine (EdU) fluorescence assays [38, 39], and western blotting analysis to determine the expression of senescence markers, p21 and p16INK4a [39]. TBHP treatment showed significantly high numbers of SA-β-gal-positive (senescent) chondrocytes, but SAC treatment showed significantly lower numbers SA-β-gal-positive chondrocytes (Figure 3A). EdU assay results showed that chondrocyte proliferation was significantly reduced by THBP but reversed by SAC in a dose-dependent manner (Figure 3B). Western blotting results showed that levels of p21 and $p16^{INK4a}$ proteins

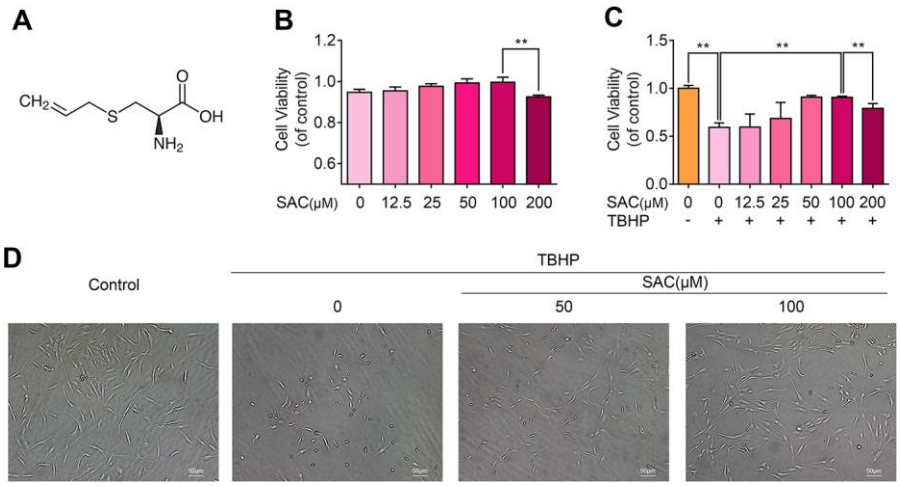

Figure 1. SAC protects chondrocytes from the cytotoxic effects of TBHP. (**A**) Chemical structure of SAC. (**B**) CCK-8 assay results show the viability of chondrocytes treated with 0, 12.5, 25, 50, 100, 200 μM SAC for 24 h. (**C**) CCK-8 assay results show the viability of chondrocytes treated with different concentrations of SAC (0, 12.5, 25, 50, 100, 200μM) for 24 h and 50 μM TBHP for 2h. (**D**) Representative phase-contrast images show the morphology of THBP-treated chondrocytes with or without SAC. Note: The data are presented as the means ± SD of five independent experiments; *$p < 0.05$, **$p < 0.01$, and ***$p < 0.001$.

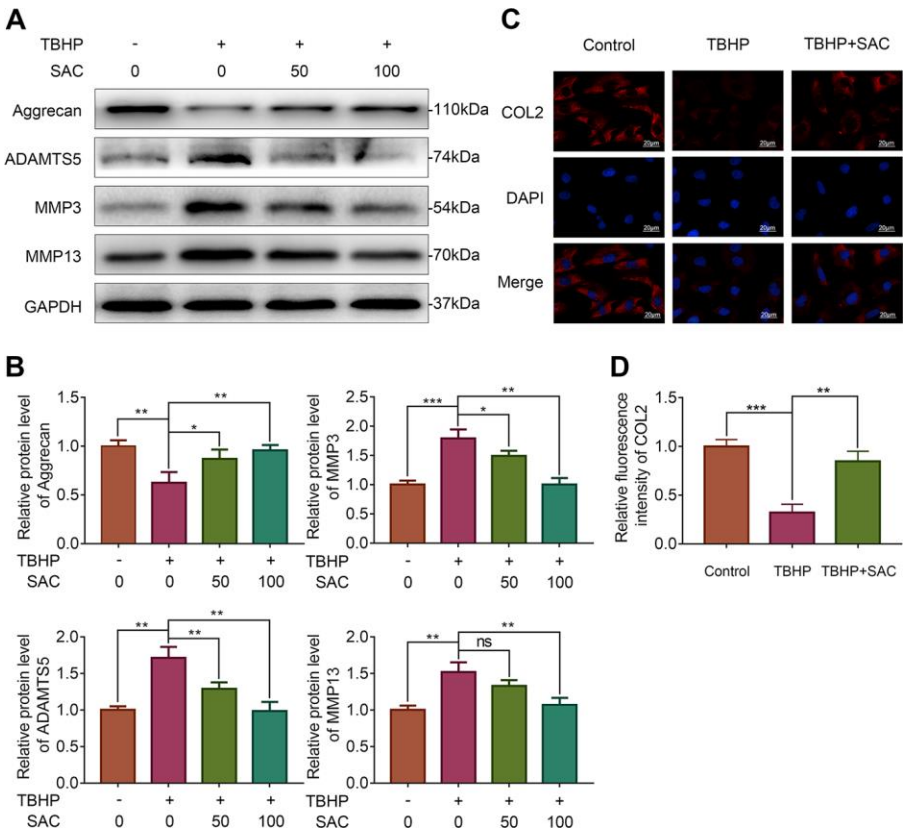

Figure 2. SAC maintain extracellular matrix homeostasis in TBHP-treated chondrocytes. (**A**) Representative images and (**B**) Histogram plots show the levels of Aggrecan, ADAMTS5, MMP3 and MMP13 proteins in chondrocytes treated with or without SAC for 24 h and stimulated with 50 μM TBHP for 2 h. (**C**) Representative immunofluorescence images show COL2 expression in chondrocytes treated with or without SAC for 24 h and 50 μM TBHP for 2 h. The nuclei were stained with DAPI. Scale bar: 20 μm. (**D**) Histogram plots show the mean fluorescence intensity of COL2 as determined from the immunofluorescence images using the Image J software. Note: The data are presented as the means ± SD of three independent experiments; *$p < 0.05$, **$p < 0.01$, and ***$p < 0.001$.

were significantly increased in the TBHP-treated chondrocytes, but were comparatively lower in SAC-treated chondrocytes (Figure 3C and 3D). These results show that SAC protects chondrocytes against TBHP-induced senescence.

SAC protects TBHP-treated chondrocytes against apoptosis

Next, we analyzed if SAC protects chondrocytes against apoptosis using the TdT-mediated dUTP Nick-End Labeling (TUNEL) assay and western blotting analysis of the expression of apoptosis-related proteins, cleaved caspase 3 (C-CASP3), BCL2 associated X (BAX) and BCL2. The numbers of TUNEL-positive chondrocytes increased upon TBHP treatment, but were significantly lower in SAC treatment groups (Figure 4A). Moreover, cleaved-caspase-3/caspase-3 ratio and BAX protein levels were increased and BCL2 protein levels were decreased in the TBHP-treated chondrocytes, but these effects were reversed by SAC treatment (Figure 4B and 4C). These results show that SAC protects chondrocytes against TBHP-induced apoptosis.

Molecular docking analysis shows that SAC interacts with the Keap1-Nrf2 complex

Next, we performed molecular docking analysis to screen candidate proteins that interact with SAC. Figure 5A shows the structure of SAC constructed using Discovery Studio 2016. The structures of potential SAC-target proteins, such as, Keap1-Nrf2 complex [40] (PDB ID: 3WN7), HDAC1 [41] (PDB ID: 4BKX), IKKβ [41] (PDB ID: 3BRV), PPARγ [42], (PDB ID: 2ATH) and TLR4 [43] (PDB ID: 2Z63), were downloaded from the Protein Data Bank (Figure 5B; Supplementary Figure 1).

Molecular docking analysis to determine the affinity between SAC and its potential targets showed high affinity interaction between SAC and the Keap1-Nrf2 complex with a -CDOCKER interaction energy value of 203.76 kcal/mol (Figure 5D and 5E; Supplementary Figure 1).

Two-dimensional (2D) binding model showed 15 van der Waals interactions, 1 alkyl interaction, and 3 carbon-hydrogen bonds between SAC and the four potential active site amino acids, namely, ARG415, ARG380, ARG483, and SER508 [44, 45] of the Keap1-Nrf2 complex (Figure 5C). Since Nrf2 forms hydrogen bonds with Keap1 amino acid residues Arg415, Arg380, Arg483, Ser508, Asn382 and Ser363 [46], these results imply that SAC may competitively inhibit the binding of Nrf2 to Keap1, which is required for its ubiquitination and subsequent degradation, and hence may be involved in activation of Nrf2. These results suggest that SAC protects chondrocytes via Nrf2.

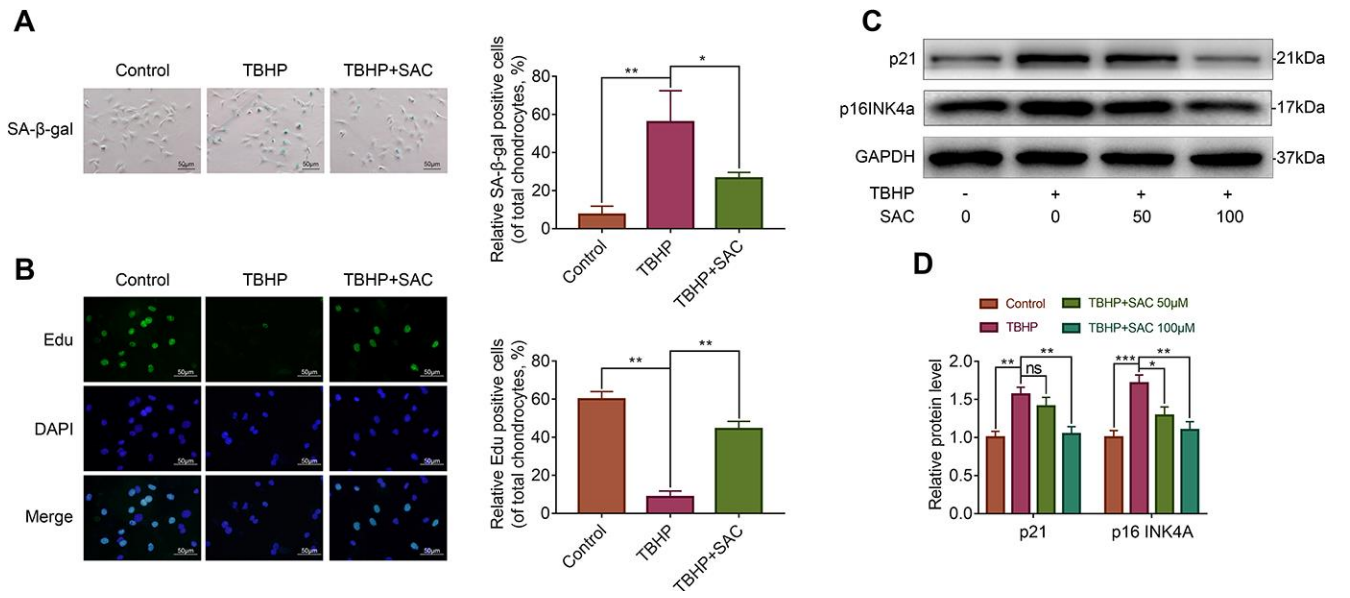

Figure 3. SAC protects TBHP-treated chondrocytes against senescence. (**A**) Representative images show the SA-β-gal staining assay results in chondrocytes treated with or without SAC for 24 h and 50 μM TBHP for 2 h. Scale bar: 50 μm. (**B**) Representative images show the EdU staining assay results in chondrocytes treated with or without SAC for 24 h and 50 μM TBHP for 2 h. Scale bar: 50 μm. (**C**) Representative western blot images and (**D**) Histogram plots show p21 and p16INK4a protein levels in chondrocytes treated with or without SAC for 24 h and 50 μM TBHP for 2 h. Note: The data are presented as the means ± SD of three independent experiments. *$p < 0.05$, **$p < 0.01$, and ***$p < 0.001$.

SAC promotes nucleus translocation of Nrf2 and activates the Nrf2 signaling pathway

Immunofluorescence analysis showed that SAC treatment resulted in the nuclear translocation of Nrf2 in the chondrocytes (Figure 6A). This was further confirmed by western blotting analysis, which showed that nuclear extracts of SAC-treated chondrocytes showed higher levels of Nrf2 compared to controls (Figure 6C and 6D). We then analyzed the expression of the Nrf2-target protein, HO1. The HO1 mRNA and protein levels were significantly higher in SAC-treated chondrocytes compared to the controls (Figure 6B and 6E). These results suggest that SAC promotes nuclear translocation of Nrf2 and activates the Nrf2/HO1 signaling pathway.

Nrf2 silencing abrogates anti-senescence and anti-apoptotic effects of SAC

To further confirm if the Nrf2/HO1 signaling pathway mediates the effects of SAC in the chondrocytes, we silenced Nrf2 using siRNAs and assessed its effects in the SAC-treated chondrocytes. Western blotting results showed that the levels of Nrf2 and HO1 proteins were significantly lower in si-Nrf2-transfected chondrocytes compared to the controls (Figure 7A and 7B). Nrf2 silencing reduced the expression of Aggrecan and increased the expression of MMP13 in SAC-treated chondrocytes compared to the controls, thereby showing dysregulation of ECM metabolic homeostasis (Figure 7C and 7D). Moreover, p21, $p16^{INK4a}$, and Bax levels were significantly higher and Bcl2 levels were significantly reduced in the Nrf2-silenced SAC-treated chondrocytes compared to controls (Figure 7E–7H). This demonstrated that Nrf2 knockdown abrogated the anti-senescence and anti-apoptotic effects of SAC in chondrocytes.

SAC ameliorates *in vivo* OA progression in DMM model mice

We established an OA model in mice by surgical destabilization of the medial meniscus (DMM) to investigate the protective effects of SAC on *in vivo* OA progression. The DMM mice were administered SAC (SAC group) or saline (DMM group) by intragastric injections, once daily for 8 weeks and the joints were analyzed by X-ray, safranin O-fast green staining and immunofluorescence.

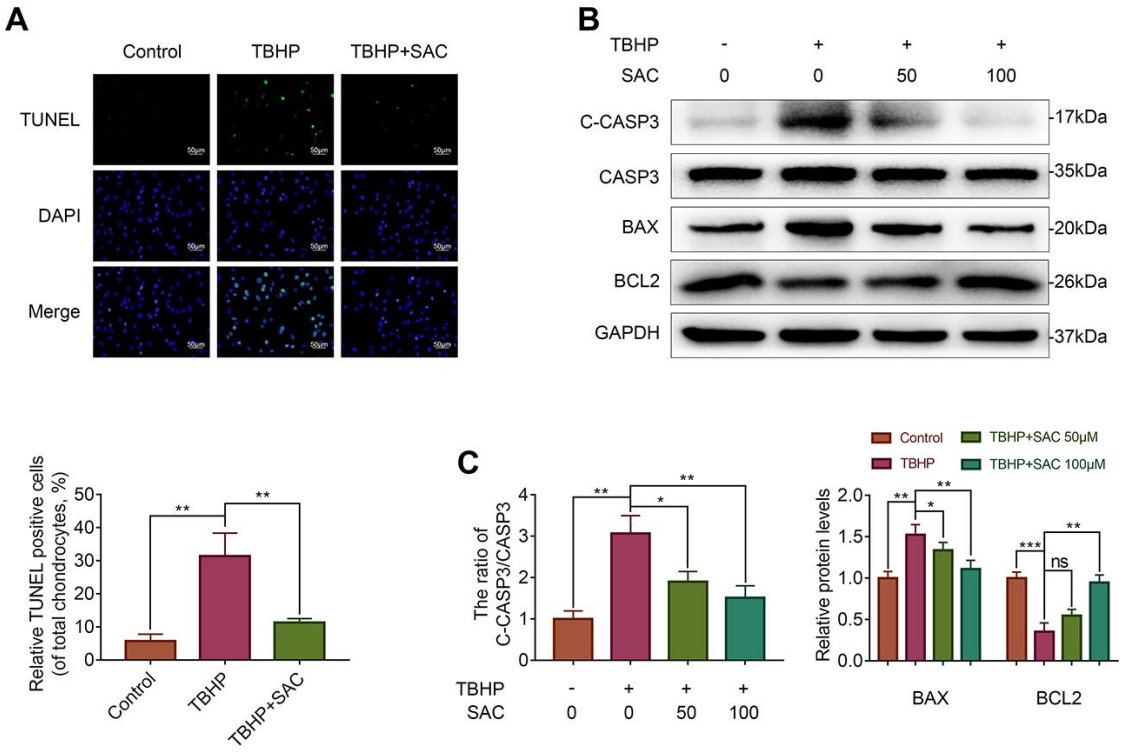

Figure 4. SAC protects TBHP-treated chondrocytes against apoptosis. (**A**) Tunel staining assay results show the number of apoptotic (Tunel-positive) chondrocytes treated with or without SAC for 24 h and 50 μM TBHP for 2 h. (**B**) Representative western blot images and (**C**) Histogram plots show the levels of cleaved-caspase3, caspase3, BAX and BCL2 proteins in the chondrocytes treated with or without SAC for 24 h and 50 μM TBHP for 2 h. Note: The data are presented as the means ± SD of three independent experiments. *$p < 0.05$, **$p < 0.01$, and ***$p < 0.001$.

X ray results showed significant cartilage ossification and severe joint-space narrowing in the DMM group, but milder cartilage ossification and joint-space narrowing in the SAC treatment group (Figure 8A). Meanwhile, OA severity was evaluated using safranin O-fast green staining of the cartilage and synovitis, and the Osteoarthritis Research Society International (OARSI) and synovitis scores. Safranin O-fast green staining showed loss of smooth cartilage articular surfaces in the DMM group, but, SAC treatment partially rescued cartilage erosion (Figure 8B). Consistent with the safranin O-fast green staining results, the OARSI scores of the DMM group were significantly higher compared to the sham and SAC groups, whereas the OARSI scores for the SAC group were higher than the DMM group but lower than the sham group (Figure 8C). Meanwhile, DMM group showed significant synovial thickening and hyper-cellularity compared to the SAC treatment group (Figure 8B and 8C).

The immunofluorescence results showed lower expression of p16INK4a and BAX in the joint cartilage sections from the SAC-treatment group compared to the DMM group, thereby suggesting that SAC treatment decreased senescence and apoptosis of the chondrocytes (Figure 8D and 8E). Furthermore, Nrf2 expression was significantly higher in the SAC group compared to the

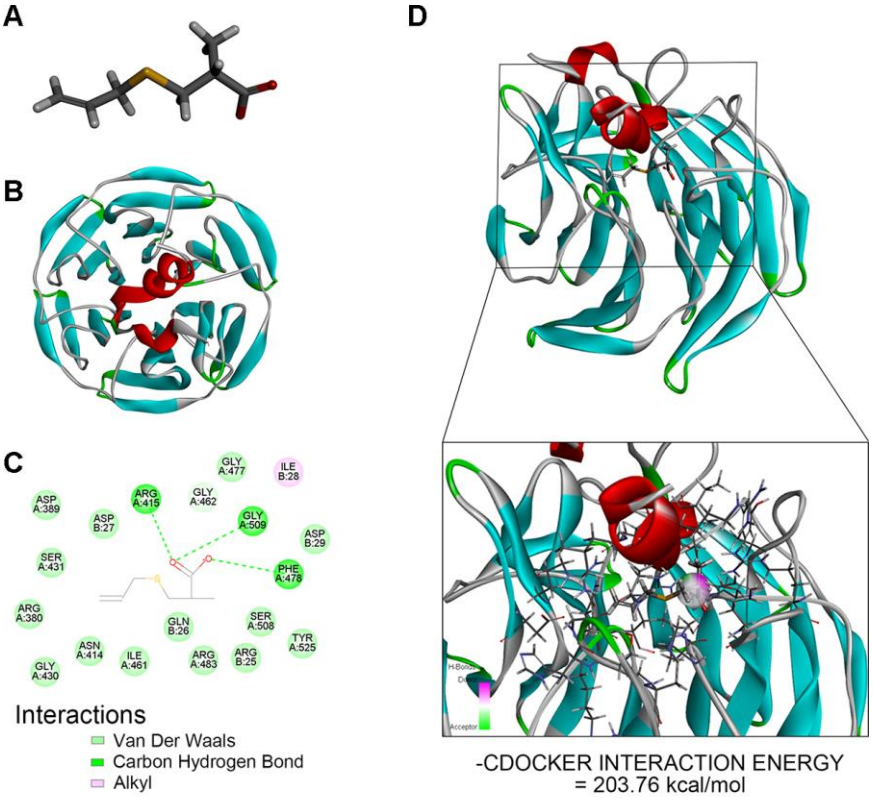

E

No	Potential targets	PDB ID	-CDOCKER_ENERGY (kcal mol-1)
1	Keap1-Nrf2 complex	3WN7	203.76
2	PPARγ	2ATH	32.06
3	IKKβ	3BRV	28.30
4	TLR4	2Z63	4.92
5	HDAC1	4BKX	4.18

Figure 5. Molecular docking analysis shows SAC interacts with the Keap1-Nrf2 complex. (**A**) The structure of SAC based on Discovery studio 2016. (**B**) The ribbon model of the Keap1-Nrf2 complex. (**C**) The 2-D model shows that Keap1-Nrf2 complex interacts with SAC through four potential active site amino acid residues, ARG415, ARG380, ARG483, and SER508. (**D**) The 3D docking model shows interactions between SAC and the Keap1-Nrf2 complex. The -CDOCKER interaction energy value for SAC and the Keap1-Nrf2 complex binding interaction was 203.76 kcal/mol. (**E**) The -CDOCKER interaction energy values for interaction between SAC and potential binding proteins, the Keap1-Nrf2 complex, HDAC1, IKKβ, PPARγ, and TLR4 are shown.

DMM group (Figure 8F and 8G). These results demonstrate that SAC attenuates senescence and apoptosis and promotes ECM homeostasis in the chondrocytes via Nrf2 activation in the *in vivo* DMM mouse model.

DISCUSSION

Osteoarthritis (OA) is a progressive and degenerative joint disease that lacks effective medications. In this study, we investigated the effects and the underlying mechanisms through which S-allyl cysteine (SAC) suppresses OA pathogenesis. We showed that SAC suppressed apoptosis and senescence in TBHP-induced chondrocytes. SAC also promotes extracellular matrix (ECM) homeostasis in TBHP -induced chondrocytes. We further demonstrate that SAC ameliorates *in vitro* and *in vivo* OA pathogenesis through Nrf2.

Previous studies have demonstrated beneficial effects of SAC in patients with Alzheimer's disease [40, 47] and chronic liver diseases [32, 48]. Therefore, we postulated that SAC may attenuate ROS-induced apoptosis, senescence and dysregulated ECM metabolism in the chondrocytes and ameliorate the progression of OA. We first observed that SAC does not induce any significant

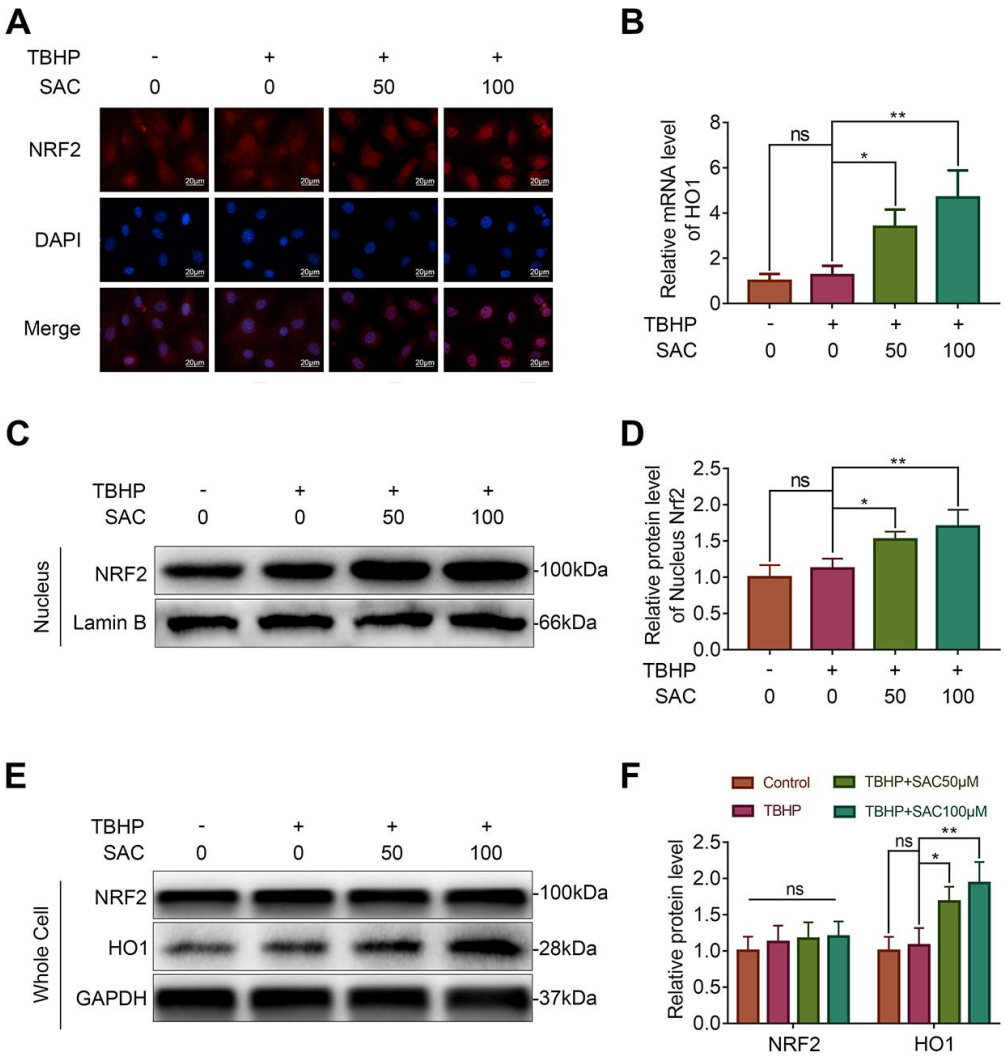

Figure 6. SAC promotes nucleus translocation of Nrf2 and activates the Nrf2/HO1 signaling pathway. (**A**) Representative immunofluorescence images show Nrf2 expression in the chondrocytes treated with or without SAC for 24 h and 50 μM TBHP for 2 h. The nuclei were stained with DAPI. Scale bar: 20 μm. (**B**) QRT-PCR analysis shows the HO1 mRNA levels in chondrocytes treated with or without SAC for 24 h and 50 μM TBHP for 2 h. (**C**) Representative western blot images and (**D**) Histogram plots show the levels of Nrf2 in the nuclei of chondrocytes treated with or without SAC for 24 h and 50 μM TBHP for 2 h. (**E**) Representative western blot images and (**F**) Histogram plots show the Nrf2 and HO1 protein levels in chondrocytes treated with or without SAC for 24 h and 50 μM TBHP for 2 h. Note: The data are presented as the means ± SD of three independent experiments. *$p < 0.05$, **$p < 0.01$, and ***$p < 0.001$.

cytotoxicity in the chondrocytes at concentrations below 100 μM. Next, we demonstrated that SAC protects TBHP-induced chondrocytes from cell death, senescence and aberrant ECM alterations.

The chondrocytes maintain an intricate balance between ECM breakdown and biosynthesis and strengthen the articular cartilage to bear tensile and compressive forces and sustain joint load and mobility [28, 49]. Our study confirms that SAC inhibits ECM breakdown and enhances ECM biosynthesis. Similar to our results, previous studies by Kim et al [50] and Zeinali et al [51] have shown that SAC significantly decreases the levels of matrix metalloproteinase-9 (MMP-9) protein, which is involved in ECM catabolism, similar to MMP3 and MMP13.

Senescent chondrocytes in the vicinity of joints are a characteristic feature of OA pathology [24, 25], and are involved in OA progression [52, 53]. Nishiyama et al showed that garlic extract prolongs the life span of senescence-accelerated mice and prevents brain atrophy [54]. In our study, SAC protects TBHP-treated chondrocytes against senescence.

Nearly 18-21% of chondrocytes are apoptotic in the OA cartilage compared to 2–5% apoptotic chondrocytes in the normal cartilage, thereby suggesting that chondrocyte apoptosis is involved in OA progression [27]. Our study demonstrates that SAC reduces apoptosis of the TBHP-treated chondrocytes. Consistent with our results, previous studies have shown that SAC suppresses cellular apoptosis to attenuate ischemia-reperfusion (I/R) injury of the cardiomyocytes [55], alcohol-related liver disease [56], and Alzheimer's disease [57]. Overall, our findings demonstrate the therapeutic potential of SAC for OA.

Molecular docking is a computational modeling method used for structure-based drug design in pharmaceutical industry because of its ability to predict the optimal binding-conformation of small molecule ligands to the target binding site [58–60]. It can also be used to elucidate fundamental biochemical processes [61, 62].

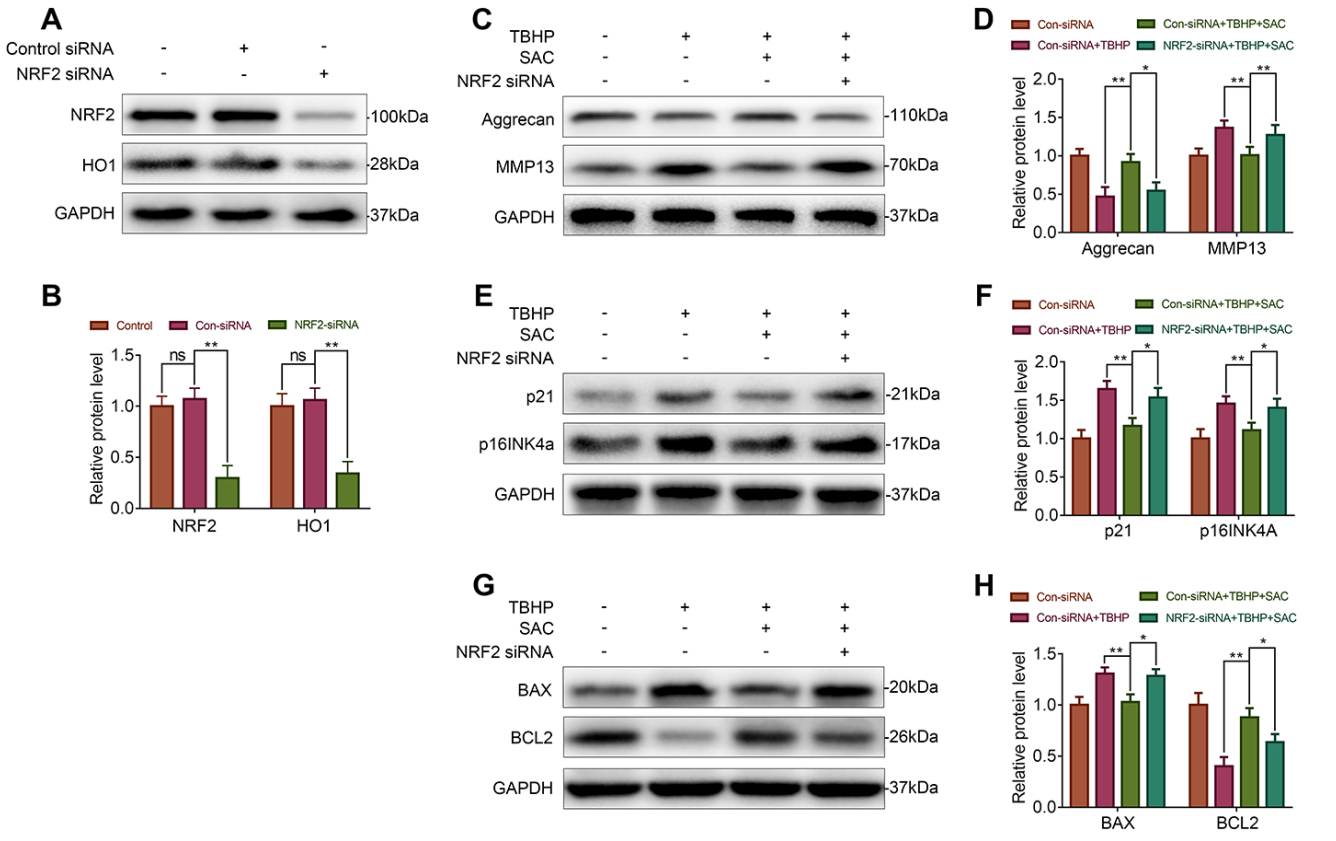

Figure 7. Nrf2 knockdown abrogates the beneficial effects of SAC. (**A**, **B**) Western blot analysis shows Nrf2 and HO1 protein levels in control and Nrf2 knockdown chondrocytes. (**C**, **E**, **G**) Representative western blot images and (**D**, **F**, **H**) Histogram plots show the levels of Aggrecan, MMP13, p21, p16INK4a, BAX, and BCL2 proteins in the control and Nrf2 knockdown chondrocytes treated with or without SAC for 24 h and 50 μM TBHP for 2 h. Note: The data are presented as the means ± SD of three independent experiments. *$p < 0.05$, **$p < 0.01$, and ***$p < 0.001$.

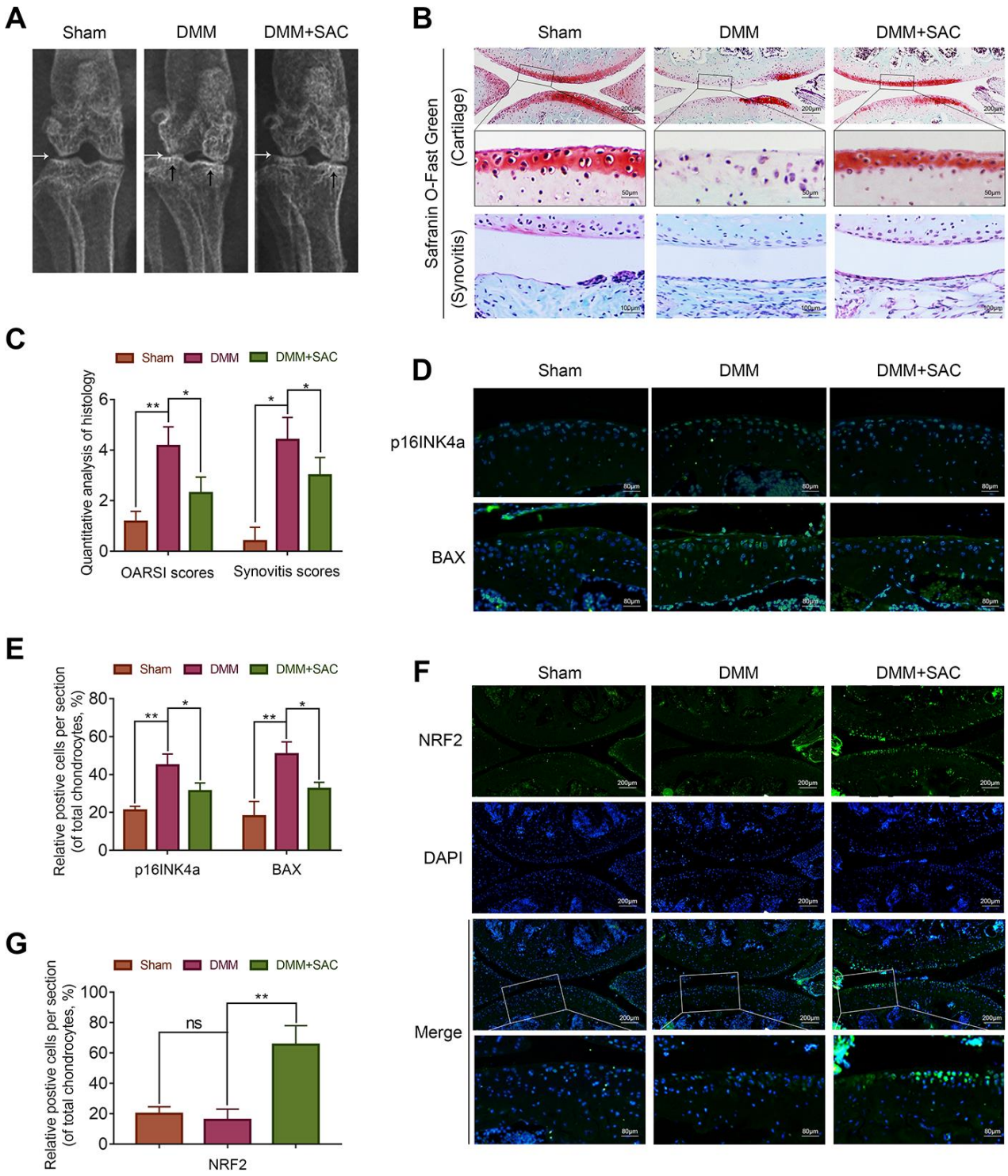

Figure 8. SAC ameliorates *in vivo* osteoarthritis progression in the DMM model mice. (**A**) Representative X-ray images show the knee joints of mice belonging to sham, DMM and DMM+SAC groups. The white arrows show the narrowing of the joint space in both the DMM and DMM+SAC mice, and the black arrows show the calcification of cartilage surface in the DMM group. (**B**) Representative images show the S-O staining of cartilage and synovitis in the knee joint sections from mice belonging to sham, DMM and DMM+SAC groups at 8-weeks post-surgery. Scale bar: 200, 50 or 100 μm. (**C**) The OARSI scores of cartilage damage and synovitis scores for the mice belonging to sham, DMM and DMM+SAC groups at 8-weeks post-surgery are shown. (**D**, **F**) Representative immunohistochemical staining images (Scale bar: 200 or 80 μm) and (**E**, **G**) Histogram plots show the levels of p16INK4a, BAX and Nrf2 proteins in the cartilage sections of mice belonging to the sham, DMM and DMM+SAC groups at 8-weeks post-surgery. Note: The data are presented as the means ± SD of five independent experiments. *$p < 0.05$, **$p < 0.01$, and ***$p < 0.001$.

In our study, molecular docking analysis identified Nrf2 as the most plausible SAC-binding target protein. Moreover, we demonstrated that SAC alleviates OA via the Nrf2 signaling pathway in the chondrocytes (Figure 5).

Nrf2 is a transcription factor that regulates antioxidant signaling pathways by binding to antioxidant response elements in the promoter regions of target genes [63]. A previous study showed that Nrf2 protein levels were significantly reduced in the cartilage tissue from OA patients compared to those from healthy individuals [64]. Oxidative stress levels and markers of articular cartilage damage were significantly elevated in Nrf2 knockout mice compared to controls [65, 66]. Although the molecular docking analysis suggests that SAC potentially interacts with Nrf2, the in vivo interactions between SAC and Nrf2 remain to be established. We demonstrate that SAC promotes nuclear localization of Nrf2 in the chondrocytes. Furthermore, knockdown of Nrf2 in chondrocytes diminishes the anti-senescent, anti-apoptotic and ECM biosynthetic effects of SAC, thereby demonstrating a key role for Nrf2 in SAC-treated chondrocytes. Similar to our results, previous studies have also shown that SAC treatment of patients with Alzheimer's disease [47], stroke [40], several chronic liver diseases [32] and diabetes mellitus [48] significantly enhances Nrf2 protein levels.

We also demonstrate the *in vivo* effects of SAC on OA pathology using the destabilized medial meniscus (DMM) mouse model [67]. In our study, DMM mice exhibit cartilage erosion and calcification, chondrocyte loss, ECM degradation, and synovitis. Furthermore, SAC treatment of DMM mice protects against cartilage degradation and synovitis. Moreover, the levels of p16INK4a and BAX are reduced in the SAC treatment group, which demonstrates further that SAC suppress *in vivo* senescence and apoptosis in chondrocytes. Meanwhile, SAC increases the levels of Nrf2 in DMM model mice. Although we did not test the effects of SAC in the Nrf2 knock-out mice, our *in vitro* results as well as the results of a previous *in vivo* study [40] suggest that SAC exerts its protective effects at least partially through Nrf2.

There are several limitations to our study. Further *in vivo* characterization and functional studies are needed to demonstrate the clinical efficacy of SAC in OA

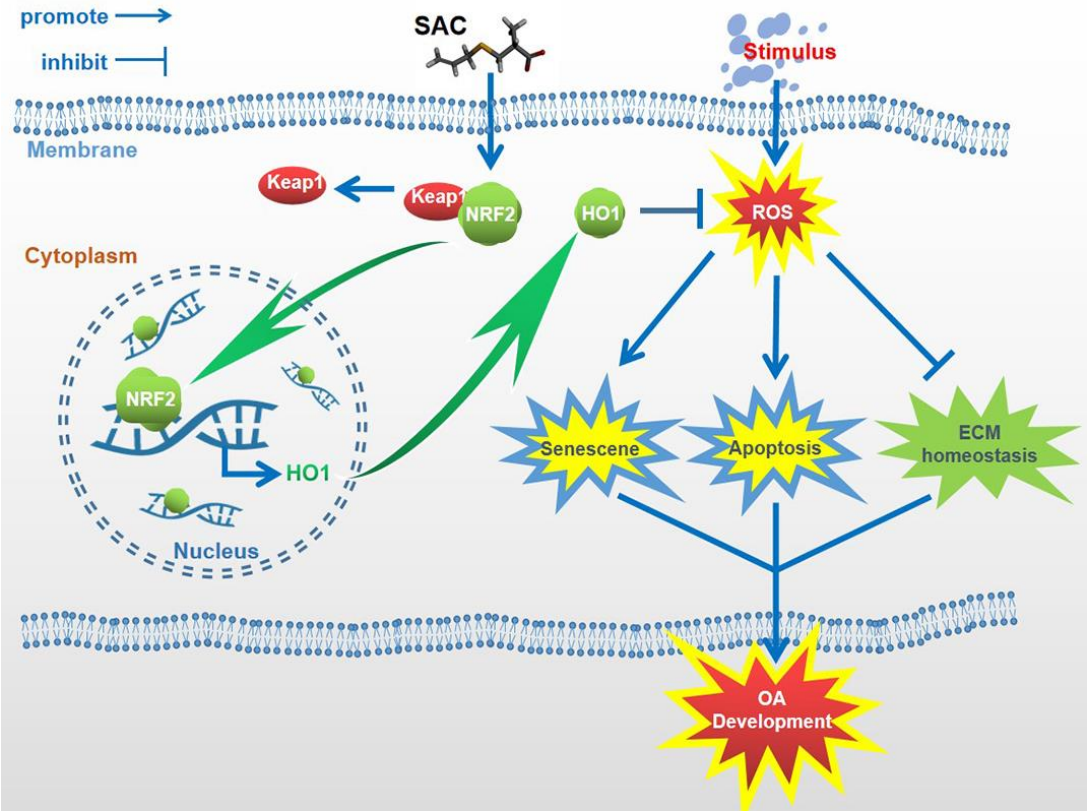

Figure 9. Schematic diagram shows the potential protective effects of SAC on OA. S-allyl cysteine suppresses senescence and apoptosis of chondrocytes and attenuates extracellular matrix metabolic dysfunction in the osteoarthritis model mice via Nrf2.

therapy. The effects of gait and pain severity need to be tested in the animal models. Gait severity analysis helps understand the behavioral changes and disease progression in preclinical arthritis models and is usually measured through observational scoring and spatio-temporal, kinetic, and kinematic measurements [68]. Moreover, Krug et al [69] demonstrated a method to measure pain in murine models by counting the number of fights and vocalizations. These tests should be included in the future studies of SAC in OA animal models and clinical studies. Another drawback of our study is that we could not establish the direct interaction between SAC and Nrf2. In the future, fluorescence or biotin-labeled SAC should be used to evaluate the direct interaction between SAC and Nrf2. Moreover, *in vivo* effects of SAC should be tested in Nrf2 knock-out mice.

Previous studies have reported an inverse association between garlic uptake and OA development [30, 31], but the mechanisms through which garlic exerts its beneficial effects on OA are yet to be discovered. Our study demonstrates that one of the active ingredients of garlic, SAC, suppresses senescence and apoptosis, and promotes extracellular matrix homeostasis in the chondrocytes. These results suggest that the large dietary intake of garlic may be replaced by smaller doses of purified SAC, but, this needs to be established in future studies. In summary, our study demonstrates that SAC suppresses OA progression in the TBHP-treated chondrocytes and the DMM model mice via the Nrf2/HO1 signaling pathway (Figure 9). Our study strongly suggests that SAC is a promising therapeutic agent to alleviate OA.

MATERIALS AND METHODS

Extraction and culture of primary mice chondrocytes

The knee cartilages of immature C57BL/6 mice were collected under aseptic conditions, cut into $1mm^3$ thick pieces, washed with phosphate-buffered saline (PBS) thrice, and digested with 0.25% type II collagenase for 4 h at 37°C. The cell suspension was centrifuged, and the cell pellet was resuspended and cultured in DMEM/F12 (Gibco) supplemented with 10% fetal bovine serum (FBS; Gibco) and 1% streptomycin/ penicillin in humidified incubator at 5% CO_2 and 37°C. The complete medium was changed every other day. The second-passage chondrocytes were used for all *in vitro* experiments.

Cell viability assay

Cell viability was analyzed using the Cell counting kit-8 (CCK-8; Dojindo, Kumamoto, Japan) according to the manufacturer's protocol. In brief, $5x10^4/cm^2$ chondrocytes were seeded in 96-well plates for 24 h, and then treated with 0, 50 or 100 μM SAC (>98% pure; Sigma-Aldrich, St Louis, MO, USA) for 24 h followed by treatment with 50 μM TBHP for 2h. Then, the cells were washed with PBS and incubated for another 2 h at 37°C with 100 μl DMEM/F12 medium containing 10 μl of CCK-8 solution. Then, the absorbance was measured at 450 nm using a microplate reader (Thermo Fisher Scientific, Rockford, USA).

Real-time PCR

Total cellular RNA was extracted using TRIzol (Invitrogen, Grand Island, NY). Then, 1μg of total RNA was reverse-transcribed using the cDNA synthesis kit (MBI Fermantas, Germany). Quantitative PCR analysis was performed using the PrimeScript-RT reagent kit (TAKARA, Japan) and SYBR Premix Ex Taq (TAKARA) in a CFX96 Real-Time PCR System (Bio-Rad Laboratories, CA, USA). The target gene expression was analyzed relative to GAPDH as an internal control using the $2^{-\Delta\Delta Ct}$ method [70].

Western blotting

Total proteins were extracted using radio immunoprecipitation assay (RIPA) buffer (Beyotime) containing 1mM phenylmethanesulfonyl fluoride (PMSF) (Beyotime), followed by centrifugation at 12,000 rpm and 4°C for 15 mins. The protein concentrations were measured using the BCA protein assay kit (Beyotime). Then, 40 ng of total protein lysates were separated using 8–12% (w/v) gradient sodium dodecyl sulfate polyacrylamide gel electrophoresis and blotted onto polyvinylidene fluoride membranes (Bio-Rad). The membranes were blocked with 5% nonfat milk for 2 h, followed by overnight incubation at 4°C with primary antibodies against BAX (1:1000; Proteintech, Wuhan, China), BCL2 (1:1000; Proteintech), Aggrecan (1:800; Abcam, Cambridge, MA, USA), ADAMTS5 (1:1000; Abcam), MMP3 (1:1000; Proteintech), MMP13 (1:1000; Proteintech), p21 (1:1000; Cell Signaling Technology, Beverly, USA), $p16^{INK4A}$ (1:800; Cell Signaling), Nrf2 (1:1000; Cell Signaling), HO1 (1:000; Cell Signaling), CASP3 (1:1000; Cell Signaling), C-CASP3 (1:800), Lamin B (1:2000; Proteintech) and GAPDH (1:2000; Proteintech). Then, the blots were incubated for 2 h at room temperature with HRP-conjugated goat anti-rabbit or goat anti-mouse IgG secondary antibodies from Bioworld (Nanjing, China). The blots were then washed thrice with Tris-buffered saline (TBS) with Tween® 20, and developed using Enhanced chemiluminescence plus reagent (Invitrogen). The protein bands were visualized using the ChemiDoc™ XRS plus imaging System (Bio-Rad) and quantified using the Image J software (Bio-Rad).

Immunofluorescence

Chondrocytes were seeded in a 6-well plate for 24 h and then treated with 0, 50 or 100 μM SAC for 24 h followed by 50 μM TBHP for 2h. Then, the chondrocytes were washed with PBS, fixed with 4% (v/v) paraformaldehyde for 15min, and permeabilized using 0.1% TritonX-100 in PBS for 10 min. Then, the cells were blocked with 5% bovine serum albumin for 1 hour at 37°, followed by overnight incubation at 4°C with primary antibodies against COL2 (1:200; Abcam) or cleaved-Caspase3 (1:150; Cell Signaling Technology). The cells were then incubated with Alexa Fluor®488- or Alexa Fluor®594-conjugated goat anti-rabbit IgG (H+L) secondary antibodies (1:300; Jackson Immunoresearch, PA, USA) for 1 hour at room temperature. Then, the cells were stained with the nuclear staining dye, DAPI (Beyotime, China) for 5 min. The stained cells were observed under a Nikon ECLIPSE Ti microscope (Nikon, Japan) and analyzed in five different random fields for each slide. The fluorescence intensity was measured using the Image J software 2.1 (Bethesda, MD, USA) and scored by observers who were blinded to the experimental groups.

EdU staining

The Click-iT EdU microplate assay kit (Invitrogen) was used according to the manufacturer's instructions to estimate the proliferation of chondrocytes based on the uptake of 5-ethynyl-2'-deoxyuridine (EdU) into the DNA. Briefly, chondrocytes from different experimental groups were incubated with EdU coupled to Oregon Green azide-conjugated EdU. Then, the cells were permeabilized and incubated with HRP-conjugated anti-Oregon Green antibody and Amplex ultrared. The stained chondrocytes were then analyzed using a fluorescence microscope (Olympus Inc).

SA-β-gal staining

Chondrocyte senescence was evaluated using the SA-β-galactosidase staining kit (Beyotime) according to manufacturer's instructions. Briefly, after treatments, chondrocytes were fixed with 0.2% glutaraldehyde for 10 minutes at room temperature and stained overnight with X-gal staining solution (pH 6.0). Then, the cells were observed under the Olympus IX71 microscope and the percentages of SA-β-gal-positive cells were estimated for all experimental and control groups.

Cell transfections

The si-Nrf2 and si-NC (negative control) were purchased from Santa Cruz Biotechnology (Dallas, TX, USA). The chondrocytes were seeded in a six-well plate and cultured for 24 h until they were 50–70% confluent. Then, the cells were transfected with 50 nM si-NC or si-Nrf2 using Lipofectamine 2000 siRNA transfection reagent (Thermo Fisher) for 48 h.

Molecular modeling

The three-dimensional structure of SAC was generated using Discovery Studio 2016 and minimized with the CHARMm force field. The structures of Keap1-Nrf2 complex (PDB ID: 3WN7) [71], HDAC1 (PDB ID: 4BKX), IKKβ (PDB ID: 3BRV), PPARγ (PDB ID: 2ATH) and TLR4 (PDB ID: 2Z63) were downloaded from the RCSB Protein Data Bank (https://www.rcsb.org/) and imported into Discovery Studio 2016. The structure of the Keap1-Nrf2 complex was then modified by removing water and adding hydrogen. The partially flexible CDOCKER program was used to determine special binding sites and the receptor radius. The molecular docking results were analyzed to determine -CDOCKER energy scores, interaction site, and interaction force types [60].

Surgical destabilization of the medial meniscus (DMM) model

The surgical interventions, treatments and postoperative animal care procedures were performed in strict accordance with the Guide for the Care and Use of Laboratory Animals of the National Institutes of Health (NIH) and as approved by the Animal Care and Use Committee of Wenzhou Medical University. Ten-week-old C57BL/6 male (n=24) wild-type (WT) mice were obtained from the Animal Center of the Chinese Academy of Sciences (Shanghai, China) and randomly divided into sham, DMM and DMM+SAC groups (n=8 mice each). Osteoarthritis was induced by surgical destabilization of the medial meniscus (DMM) as previously described [67]. Briefly, the mice belonging to the DMM and DMM+SAC groups were anesthetized with an intraperitoneal injection of 2% w/v pentobarbital (40 mg/kg). Then, the joint capsule of the right knee just medial to the patellar tendon was incised and spread open. The medial meniscotibial ligament was also transected with the microsurgical scissors. In the sham group, arthrotomy was performed without the transection of the medial meniscotibial ligament. The mice in the sham and DMM groups were administered saline every day through intragastric injections, whereas mice in the DMM+SAC group received 100 mg/kg/day SAC dissolved in saline through intragastric injections as previously described [72]. The mice were killed 2 months after surgery, and the knee joints were collected for imaging and histological analysis.

X-ray imaging analysis

The Kubtec XPERT 80 Digital X-ray machine (KUB Technologies Inc., Connecticut, USA) was used for imaging at 50 Kv and 160 μA to evaluate the joint space and the calcification changes in the cartilage surface in all the mice at 8 weeks after surgery.

Histopathological analysis

The joint specimens from the 3 groups of mice were subjected to safranin O-fast green staining. A separate group of experienced histology researchers examined the cellularity and morphology of the cartilage and subchondral bone using a Olympus light microscope (Olympus Inc.) in a blinded fashion and estimated the scores based on the Osteoarthritis Research Society International (OARSI) scoring system for the medial femoral condyle and medial tibial plateau as described previously [73]. The severity of synovitis was graded using a scoring system as previously described [74].

Statistical analysis

The data are presented as means ± standard deviation (S.D) from three independent experiments. Statistical analysis was performed using the SPSS 20.0 statistical software (IBM, Armonk, NY, USA). Parametric data was compared using the one-way analysis of variance (ANOVA) and Tukey's post hoc test. Nonparametric data (OARSI scores and synovitis scores) was analyzed using the Kruskal–Wallis H test. $P < 0.05$ was considered statistically significant.

AUTHOR CONTRIBUTIONS

ZP, YZ, XZ and XW designed the study; ZS, JL, QZ and YW performed *in vitro* experiments; ZS wrote the manuscript; LB, SF and YW conducted the *in vivo* experiments; NT, WG and LS provided materials and methods; FG revised the manuscript. All authors consented to the final manuscript.

ACKNOWLEDGMENTS

This work was financially supported by the Zhejiang Provincial Natural Science Foundation of China (Grant No. LQ19H060004), Wenzhou Science and Technology Bureau Foundation (Grant No. ZY2019014), and the National Natural Science Foundation of China (Grant No.81871806).

CONFLICTS OF INTEREST

The authors confirm that there are no conflicts of interest.

REFERENCES

1. Cross M, Smith E, Hoy D, Nolte S, Ackerman I, Fransen M, Bridgett L, Williams S, Guillemin F, Hill CL, Laslett LL, Jones G, Cicuttini F, et al. The global burden of hip and knee osteoarthritis: estimates from the global burden of disease 2010 study. Ann Rheum Dis. 2014; 73:1323–30. https://doi.org/10.1136/annrheumdis-2013-204763 PMID:24553908

2. Hunter DJ, Bierma-Zeinstra S. Osteoarthritis. Lancet. 2019; 393:1745–59. https://doi.org/10.1016/S0140-6736(19)30417-9 PMID:31034380

3. Neogi T, Zhang Y. Epidemiology of osteoarthritis. Rheum Dis Clin North Am. 2013; 39:1–19. https://doi.org/10.1016/j.rdc.2012.10.004 PMID:23312408

4. Huey DJ, Hu JC, Athanasiou KA. Unlike bone, cartilage regeneration remains elusive. Science. 2012; 338:917–21. https://doi.org/10.1126/science.1222454 PMID:23161992

5. Djouad F, Bouffi C, Ghannam S, Noël D, Jorgensen C. Mesenchymal stem cells: innovative therapeutic tools for rheumatic diseases. Nat Rev Rheumatol. 2009; 5:392–99. https://doi.org/10.1038/nrrheum.2009.104 PMID:19568253

6. Lepetsos P, Papavassiliou AG. ROS/oxidative stress signaling in osteoarthritis. Biochim Biophys Acta. 2016; 1862:576–91. https://doi.org/10.1016/j.bbadis.2016.01.003 PMID:26769361

7. Yao Y, Zhang H, Wang Z, Ding J, Wang S, Huang B, Ke S, Gao C. Reactive Oxygen Species (ROS)-responsive biomaterials mediate tissue microenvironments and tissue regeneration. J Mater Chem B. 2019; 7:5019–37. https://doi.org/10.1039/c9tb00847k PMID:31432870

8. Bolduc JA, Collins JA, Loeser RF. Reactive oxygen species, aging and articular cartilage homeostasis. Free Radic Biol Med. 2019; 132:73–82. https://doi.org/10.1016/j.freeradbiomed.2018.08.038 PMID:30176344

9. Koike M, Nojiri H, Ozawa Y, Watanabe K, Muramatsu Y, Kaneko H, Morikawa D, Kobayashi K, Saita Y, Sasho T, Shirasawa T, Yokote K, Kaneko K, Shimizu T. Mechanical overloading causes mitochondrial superoxide and SOD2 imbalance in chondrocytes resulting in cartilage degeneration. Sci Rep. 2015; 5:11722. https://doi.org/10.1038/srep11722 PMID:26108578

10. Aigner T, Fundel K, Saas J, Gebhard PM, Haag J, Weiss T, Zien A, Obermayr F, Zimmer R, Bartnik E. Large-scale gene expression profiling reveals major pathogenetic pathways of cartilage degeneration in osteoarthritis. Arthritis Rheum. 2006; 54:3533–44. https://doi.org/10.1002/art.22174 PMID:17075858

11. Chistiakov DA, Sobenin IA, Revin VV, Orekhov AN, Bobryshev YV. Mitochondrial aging and age-related dysfunction of mitochondria. Biomed Res Int. 2014; 2014:238463. https://doi.org/10.1155/2014/238463 PMID:24818134

12. Doll DN, Rellick SL, Barr TL, Ren X, Simpkins JW. Rapid mitochondrial dysfunction mediates TNF-alpha-induced neurotoxicity. J Neurochem. 2015; 132:443–51. https://doi.org/10.1111/jnc.13008 PMID:25492727

13. Yuan D, Huang S, Berger E, Liu L, Gross N, Heinzmann F, Ringelhan M, Connor TO, Stadler M, Meister M, Weber J, Öllinger R, Simonavicius N, et al. Kupffer cell-derived tnf triggers cholangiocellular tumorigenesis through JNK due to chronic mitochondrial dysfunction and ROS. Cancer Cell. 2017; 31:771–89.e6. https://doi.org/10.1016/j.ccell.2017.05.006 PMID:28609656

14. Da Sylva TR, Connor A, Mburu Y, Keystone E, Wu GE. Somatic mutations in the mitochondria of rheumatoid arthritis synoviocytes. Arthritis Res Ther. 2005; 7:R844–51. https://doi.org/10.1186/ar1752 PMID:15987486

15. Grishko VI, Ho R, Wilson GL, Pearsall AW 4th. Diminished mitochondrial DNA integrity and repair capacity in OA chondrocytes. Osteoarthritis Cartilage. 2009; 17:107–13. https://doi.org/10.1016/j.joca.2008.05.009 PMID:18562218

16. Yudoh K, Nguyen vT, Nakamura H, Hongo-Masuko K, Kato T, Nishioka K. Potential involvement of oxidative stress in cartilage senescence and development of osteoarthritis: oxidative stress induces chondrocyte telomere instability and downregulation of chondrocyte function. Arthritis Res Ther. 2005; 7:R380–91. https://doi.org/10.1186/ar1499 PMID:15743486

17. Martin JA, Klingelhutz AJ, Moussavi-Harami F, Buckwalter JA. Effects of oxidative damage and telomerase activity on human articular cartilage chondrocyte senescence. J Gerontol A Biol Sci Med Sci. 2004; 59:324–37. https://doi.org/10.1093/gerona/59.4.b324 PMID:15071075

18. Green DR, Kroemer G. The pathophysiology of mitochondrial cell death. Science. 2004; 305:626–29. https://doi.org/10.1126/science.1099320 PMID:15286356

19. Mazat JP, Ransac S, Heiske M, Devin A, Rigoulet M. Mitochondrial energetic metabolism-some general principles. IUBMB Life. 2013; 65:171–79. https://doi.org/10.1002/iub.1138 PMID:23441039

20. Tiku ML, Gupta S, Deshmukh DR. Aggrecan degradation in chondrocytes is mediated by reactive oxygen species and protected by antioxidants. Free Radic Res. 1999; 30:395–405. https://doi.org/10.1080/10715769900300431 PMID:10342332

21. Yu H, Ye WB, Zhong ZM, Ding RT, Chen JT. Effect of advanced oxidation protein products on articular cartilage and synovium in a rabbit osteoarthritis model. Orthop Surg. 2015; 7:161–67. https://doi.org/10.1111/os.12179 PMID:26033998

22. Ge Z, Hu Y, Heng BC, Yang Z, Ouyang H, Lee EH, Cao T. Osteoarthritis and therapy. Arthritis Rheum. 2006; 55:493–500. https://doi.org/10.1002/art.21994 PMID:16739189

23. Malfait AM. Osteoarthritis year in review 2015: biology. Osteoarthritis Cartilage. 2016; 24:21–26. https://doi.org/10.1016/j.joca.2015.09.010 PMID:26707989

24. Lotz M, Loeser RF. Effects of aging on articular cartilage homeostasis. Bone. 2012; 51:241–48. https://doi.org/10.1016/j.bone.2012.03.023 PMID:22487298

25. Mobasheri A, Matta C, Zákány R, Musumeci G. Chondrosenescence: definition, hallmarks and potential role in the pathogenesis of osteoarthritis. Maturitas. 2015; 80:237–44. https://doi.org/10.1016/j.maturitas.2014.12.003 PMID:25637957

26. Lane NE, Brandt K, Hawker G, Peeva E, Schreyer E, Tsuji W, Hochberg MC. OARSI-FDA initiative: defining the disease state of osteoarthritis. Osteoarthritis Cartilage. 2011; 19:478–82. https://doi.org/10.1016/j.joca.2010.09.013 PMID:21396464

27. Héraud F, Héraud A, Harmand MF. Apoptosis in normal and osteoarthritic human articular cartilage. Ann Rheum Dis. 2000; 59:959–65. https://doi.org/10.1136/ard.59.12.959 PMID:11087699

28. Goldring MB. The role of the chondrocyte in osteoarthritis. Arthritis Rheum. 2000; 43:1916–26. https://doi.org/10.1002/1529-0131(200009)43:9<1916::AID-ANR2>3.0.CO;2-I PMID:11014341

29. Chen J, Xie JJ, Shi KS, Gu YT, Wu CC, Xuan J, Ren Y, Chen L, Wu YS, Zhang XL, Xiao J, Wang DZ, Wang XY. Glucagon-like peptide-1 receptor regulates endoplasmic reticulum stress-induced apoptosis and the associated inflammatory response in chondrocytes and the progression of osteoarthritis in rat. Cell Death Dis. 2018; 9:212. https://doi.org/10.1038/s41419-017-0217-y PMID:29434185

30. Williams FM, Skinner J, Spector TD, Cassidy A, Clark IM, Davidson RM, MacGregor AJ. Dietary garlic and hip osteoarthritis: evidence of a protective effect and putative mechanism of action. BMC Musculoskelet Disord. 2010; 11:280. https://doi.org/10.1186/1471-2474-11-280 PMID:21143861

31. Dehghani S, Alipoor E, Salimzadeh A, Yaseri M, Hosseini M, Feinle-Bisset C, Hosseinzadeh-Attar MJ. The effect of a garlic supplement on the pro-inflammatory adipocytokines, resistin and tumor necrosis factor-alpha, and on pain severity, in overweight or obese women with knee osteoarthritis. Phytomedicine. 2018; 48:70–75. https://doi.org/10.1016/j.phymed.2018.04.060 PMID:30195882

32. Basu C, Sur R. S-allyl cysteine alleviates hydrogen peroxide induced oxidative injury and apoptosis through upregulation of Akt/Nrf-2/HO-1 signaling pathway in HepG2 cells. Biomed Res Int. 2018; 2018:3169431. https://doi.org/10.1155/2018/3169431 PMID:30515391

33. Javed H, Khan MM, Khan A, Vaibhav K, Ahmad A, Khuwaja G, Ahmed ME, Raza SS, Ashafaq M, Tabassum R, Siddiqui MS, El-Agnaf OM, Safhi MM, Islam F. S-allyl cysteine attenuates oxidative stress associated cognitive impairment and neurodegeneration in mouse model of streptozotocin-induced experimental dementia of Alzheimer's type. Brain Res. 2011; 1389:133–42. https://doi.org/10.1016/j.brainres.2011.02.072 PMID:21376020

34. Khajevand-Khazaei MR, Azimi S, Sedighnejad L, Salari S, Ghorbanpour A, Baluchnejadmojarad T, Mohseni-Moghaddam P, Khamse S, Roghani M. S-allyl cysteine protects against lipopolysaccharide-induced acute kidney injury in the C57BL/6 mouse strain: involvement of oxidative stress and inflammation. Int Immunopharmacol. 2019; 69:19–26. https://doi.org/10.1016/j.intimp.2019.01.026 PMID:30665040

35. Park JM, Han YM, Kangwan N, Lee SY, Jung MK, Kim EH, Hahm KB. S-allyl cysteine alleviates nonsteroidal anti-inflammatory drug-induced gastric mucosal damages by increasing cyclooxygenase-2 inhibition, heme oxygenase-1 induction, and histone deacetylation inhibition. J Gastroenterol Hepatol. 2014 (Suppl 4); 29:80–92. https://doi.org/10.1111/jgh.12730 PMID:25521739

36. Zheng G, Pan Z, Zhan Y, Tang Q, Zheng F, Zhou Y, Wu Y, Zhou Y, Chen D, Chen J, Wang X, Gao W, Xu H, et al. TFEB protects nucleus pulposus cells against apoptosis and senescence via restoring autophagic flux. Osteoarthritis Cartilage. 2019; 27:347–57. https://doi.org/10.1016/j.joca.2018.10.011 PMID:30414849

37. Zhang Z, Lin J, Tian N, Wu Y, Zhou Y, Wang C, Wang Q, Jin H, Chen T, Nisar M, Zheng G, Xu T, Gao W, et al. Melatonin protects vertebral endplate chondrocytes against apoptosis and calcification via the Sirt1-autophagy pathway. J Cell Mol Med. 2019; 23:177–93. https://doi.org/10.1111/jcmm.13903 PMID:30353656

38. Chen Y, Lin J, Chen J, Huang C, Zhang Z, Wang J, Wang K, Wang X. Mfn2 is involved in intervertebral disc degeneration through autophagy modulation. Osteoarthritis Cartilage. 2020; 28:363–74. https://doi.org/10.1016/j.joca.2019.12.009 PMID:31926268

39. Chen J, Xie JJ, Jin MY, Gu YT, Wu CC, Guo WJ, Yan YZ, Zhang ZJ, Wang JL, Zhang XL, Lin Y, Sun JL, Zhu GH, et al. Sirt6 overexpression suppresses senescence and apoptosis of nucleus pulposus cells by inducing autophagy in a model of intervertebral disc degeneration. Cell Death Dis. 2018; 9:56. https://doi.org/10.1038/s41419-017-0085-5 PMID:29352194

40. Shi H, Jing X, Wei X, Perez RG, Ren M, Zhang X, Lou H. S-allyl cysteine activates the Nrf2-dependent antioxidant response and protects neurons against ischemic injury in vitro and in vivo. J Neurochem. 2015; 133:298–308. https://doi.org/10.1111/jnc.12986 PMID:25393425

41. Aggarwal BB, Shishodia S. Molecular targets of dietary agents for prevention and therapy of cancer. Biochem Pharmacol. 2006; 71:1397–421. https://doi.org/10.1016/j.bcp.2006.02.009 PMID:16563357

42. Wang YL, Guo XY, He W, Chen RJ, Zhuang R. Effects of alliin on LPS-induced acute lung injury by activating PPARγ. Microb Pathog. 2017; 110:375–79. https://doi.org/10.1016/j.micpath.2017.07.019 PMID:28711511

43. Zarezadeh M, Baluchnejadmojarad T, Kiasalari Z, Afshin-Majd S, Roghani M. Garlic active constituent s-allyl cysteine protects against lipopolysaccharide-

induced cognitive deficits in the rat: possible involved mechanisms. Eur J Pharmacol. 2017; 795:13–21. https://doi.org/10.1016/j.ejphar.2016.11.051 PMID:27915041

44. Davies TG, Wixted WE, Coyle JE, Griffiths-Jones C, Hearn K, McMenamin R, Norton D, Rich SJ, Richardson C, Saxty G, Willems HM, Woolford AJ, Cottom JE, et al. Monoacidic inhibitors of the kelch-like ECH-associated protein 1: nuclear factor erythroid 2-related factor 2 (KEAP1:NRF2) protein-protein interaction with high cell potency identified by fragment-based discovery. J Med Chem. 2016; 59:3991–4006. https://doi.org/10.1021/acs.jmedchem.6b00228 PMID:27031670

45. Fukutomi T, Takagi K, Mizushima T, Ohuchi N, Yamamoto M. Kinetic, thermodynamic, and structural characterizations of the association between Nrf2-DLGex degron and Keap1. Mol Cell Biol. 2014; 34:832–46. https://doi.org/10.1128/MCB.01191-13 PMID:24366543

46. Canning P, Sorrell FJ, Bullock AN. Structural basis of Keap1 interactions with Nrf2. Free Radic Biol Med. 2015; 88:101–07. https://doi.org/10.1016/j.freeradbiomed.2015.05.034 PMID:26057936

47. Denzer I, Münch G, Pischetsrieder M, Friedland K. S-allyl-L-cysteine and isoliquiritigenin improve mitochondrial function in cellular models of oxidative and nitrosative stress. Food Chem. 2016; 194:843–48. https://doi.org/10.1016/j.foodchem.2015.08.052 PMID:26471626

48. Baluchnejadmojarad T, Kiasalari Z, Afshin-Majd S, Ghasemi Z, Roghani M. S-allyl cysteine ameliorates cognitive deficits in streptozotocin-diabetic rats via suppression of oxidative stress, inflammation, and acetylcholinesterase. Eur J Pharmacol. 2017; 794:69–76. https://doi.org/10.1016/j.ejphar.2016.11.033 PMID:27887948

49. Goldring MB. Osteoarthritis and cartilage: the role of cytokines. Curr Rheumatol Rep. 2000; 2:459–65. https://doi.org/10.1007/s11926-000-0021-y PMID:11123098

50. Kim SR, Jung YR, An HJ, Kim DH, Jang EJ, Choi YJ, Moon KM, Park MH, Park CH, Chung KW, Bae HR, Choi YW, Kim ND, Chung HY. Anti-wrinkle and anti-inflammatory effects of active garlic components and the inhibition of MMPs via NF-κB signaling. PLoS One. 2013; 8:e73877. https://doi.org/10.1371/journal.pone.0073877 PMID:24066081

51. Zeinali H, Baluchnejadmojarad T, Fallah S, Sedighi M, Moradi N, Roghani M. S-allyl cysteine improves clinical and neuropathological features of experimental autoimmune encephalomyelitis in C57BL/6 mice. Biomed Pharmacother. 2018; 97:557–63. https://doi.org/10.1016/j.biopha.2017.10.155 PMID:29101799

52. McCulloch K, Litherland GJ, Rai TS. Cellular senescence in osteoarthritis pathology. Aging Cell. 2017; 16:210–18. https://doi.org/10.1111/acel.12562 PMID:28124466

53. Jeon OH, Kim C, Laberge RM, Demaria M, Rathod S, Vasserot AP, Chung JW, Kim DH, Poon Y, David N, Baker DJ, van Deursen JM, Campisi J, Elisseeff JH. Local clearance of senescent cells attenuates the development of post-traumatic osteoarthritis and creates a pro-regenerative environment. Nat Med. 2017; 23:775–81. https://doi.org/10.1038/nm.4324 PMID:28436958

54. Nishiyama N, Moriguchi T, Morihara N, Saito H. Ameliorative effect of s-allylcysteine, a major thioallyl constituent in aged garlic extract, on learning deficits in senescence-accelerated mice. J Nutr. 2001; 131:1093S–5S. https://doi.org/10.1093/jn/131.3.1093S PMID:11238823

55. Zhao R, Xie E, Yang X, Gong B. Alliin alleviates myocardial ischemia-reperfusion injury by promoting autophagy. Biochem Biophys Res Commun. 2019; 512:236–43. https://doi.org/10.1016/j.bbrc.2019.03.046 PMID:30885435

56. Chen P, Hu M, Liu F, Yu H, Chen C. S-allyl-l-cysteine (SAC) protects hepatocytes from alcohol-induced apoptosis. FEBS Open Bio. 2019; 9:1327–36. https://doi.org/10.1002/2211-5463.12684 PMID:31161729

57. Peng Q, Buz'Zard AR, Lau BH. Neuroprotective effect of garlic compounds in amyloid-beta peptide-induced apoptosis in vitro. Med Sci Monit. 2002; 8:BR328–37. PMID:12165737

58. Maji B, Bhattacharya S. Advances in the molecular design of potential anticancer agents via targeting of human telomeric DNA. Chem Commun (Camb). 2014; 50:6422–38. https://doi.org/10.1039/c4cc00611a PMID:24695755

59. Khan NM, Haseeb A, Ansari MY, Devarapalli P, Haynie S, Haqqi TM. Wogonin, a plant derived small molecule, exerts potent anti-inflammatory and chondroprotective effects through the activation of ROS/ERK/Nrf2 signaling pathways in human

Osteoarthritis chondrocytes. Free Radic Biol Med. 2017; 106:288–301. https://doi.org/10.1016/j.freeradbiomed.2017.02.041 PMID:28237856

60. Tu M, Liu H, Zhang R, Chen H, Mao F, Cheng S, Lu W, Du M. Analysis and Evaluation of the Inhibitory Mechanism of a Novel Angiotensin-I-Converting Enzyme Inhibitory Peptide Derived from Casein Hydrolysate. J Agric Food Chem. 2018; 66:4139–4144. https://doi.org/10.1021/acs.jafc.8b00732 PMID:29637780

61. Kitchen DB, Decornez H, Furr JR, Bajorath J. Docking and scoring in virtual screening for drug discovery: methods and applications. Nat Rev Drug Discov. 2004; 3:935–49. https://doi.org/10.1038/nrd1549 PMID:15520816

62. Srivastava P, Tiwari A. Critical role of computer simulations in drug discovery and development. Curr Top Med Chem. 2017; 17:2422–32. https://doi.org/10.2174/1568026617666170403113541 PMID:28366137

63. Motohashi H, Yamamoto M. Nrf2-Keap1 defines a physiologically important stress response mechanism. Trends Mol Med. 2004; 10:549–57. https://doi.org/10.1016/j.molmed.2004.09.003 PMID:15519281

64. Wang Y, Zhao X, Lotz M, Terkeltaub R, Liu-Bryan R. Mitochondrial biogenesis is impaired in osteoarthritis chondrocytes but reversible via peroxisome proliferator-activated receptor γ coactivator 1α. Arthritis Rheumatol. 2015; 67:2141–53. https://doi.org/10.1002/art.39182 PMID:25940958

65. Wruck CJ, Fragoulis A, Gurzynski A, Brandenburg LO, Kan YW, Chan K, Hassenpflug J, Freitag-Wolf S, Varoga D, Lippross S, Pufe T. Role of oxidative stress in rheumatoid arthritis: insights from the Nrf2-knockout mice. Ann Rheum Dis. 2011; 70:844–50. https://doi.org/10.1136/ard.2010.132720 PMID:21173018

66. Cai D, Yin S, Yang J, Jiang Q, Cao W. Histone deacetylase inhibition activates Nrf2 and protects against osteoarthritis. Arthritis Res Ther. 2015; 17:269. https://doi.org/10.1186/s13075-015-0774-3 PMID:26408027

67. Glasson SS, Blanchet TJ, Morris EA. The surgical destabilization of the medial meniscus (DMM) model of osteoarthritis in the 129/SvEv mouse. Osteoarthritis Cartilage. 2007; 15:1061–69. https://doi.org/10.1016/j.joca.2007.03.006 PMID:17470400

68. Lakes EH, Allen KD. Gait analysis methods for rodent models of arthritic disorders: reviews and recommendations. Osteoarthritis Cartilage. 2016; 24:1837–49. https://doi.org/10.1016/j.joca.2016.03.008 PMID:26995111

69. Krug HE, Dorman C, Blanshan N, Frizelle S, Mahowald M. Spontaneous and evoked measures of pain in murine models of monoarticular knee pain. J Vis Exp. 2019. [Epub ahead of print]. https://doi.org/10.3791/59024 PMID:30855579

70. Pfaffl MW. A new mathematical model for relative quantification in real-time RT-PCR. Nucleic Acids Res. 2001; 29:e45. https://doi.org/10.1093/nar/29.9.e45 PMID:11328886

71. Tsou HR, MacEwan G, Birnberg G, Grosu G, Bursavich MG, Bard J, Brooijmans N, Toral-Barza L, Hollander I, Mansour TS, Ayral-Kaloustian S, Yu K. Discovery and optimization of 2-(4-substituted-pyrrolo[2,3-b]pyridin-3-yl)methylene-4-hydroxybenzofuran-3(2H)-ones as potent and selective ATP-competitive inhibitors of the mammalian target of rapamycin (mTOR). Bioorg Med Chem Lett. 2010; 20:2321–5. https://doi.org/10.1016/j.bmcl.2010.01.135 PMID:20188552

72. Zhao L, Wu D, Sang M, Xu Y, Liu Z, Wu Q. Stachydrine ameliorates isoproterenol-induced cardiac hypertrophy and fibrosis by suppressing inflammation and oxidative stress through inhibiting NF-κB and JAK/STAT signaling pathways in rats. Int Immunopharmacol. 2017; 48:102–09. https://doi.org/10.1016/j.intimp.2017.05.002 PMID:28499193

73. Kraus VB, Huebner JL, DeGroot J, Bendele A. The OARSI histopathology initiative - recommendations for histological assessments of osteoarthritis in the Guinea pig. Osteoarthritis Cartilage. 2010 (Suppl 3); 18:S35–52. https://doi.org/10.1016/j.joca.2010.04.015 PMID:20864022

74. Tang S, Tang Q, Jin J, Zheng G, Xu J, Huang W, Li X, Shang P, Liu H. Polydatin inhibits the IL-1β-induced inflammatory response in human osteoarthritic chondrocytes by activating the Nrf2 signaling pathway and ameliorates murine osteoarthritis. Food Funct. 2018; 9:1701–12. https://doi.org/10.1039/c7fo01555k PMID:29484338

SUPPLEMENTARY MATERIALS

Supplementary Figures

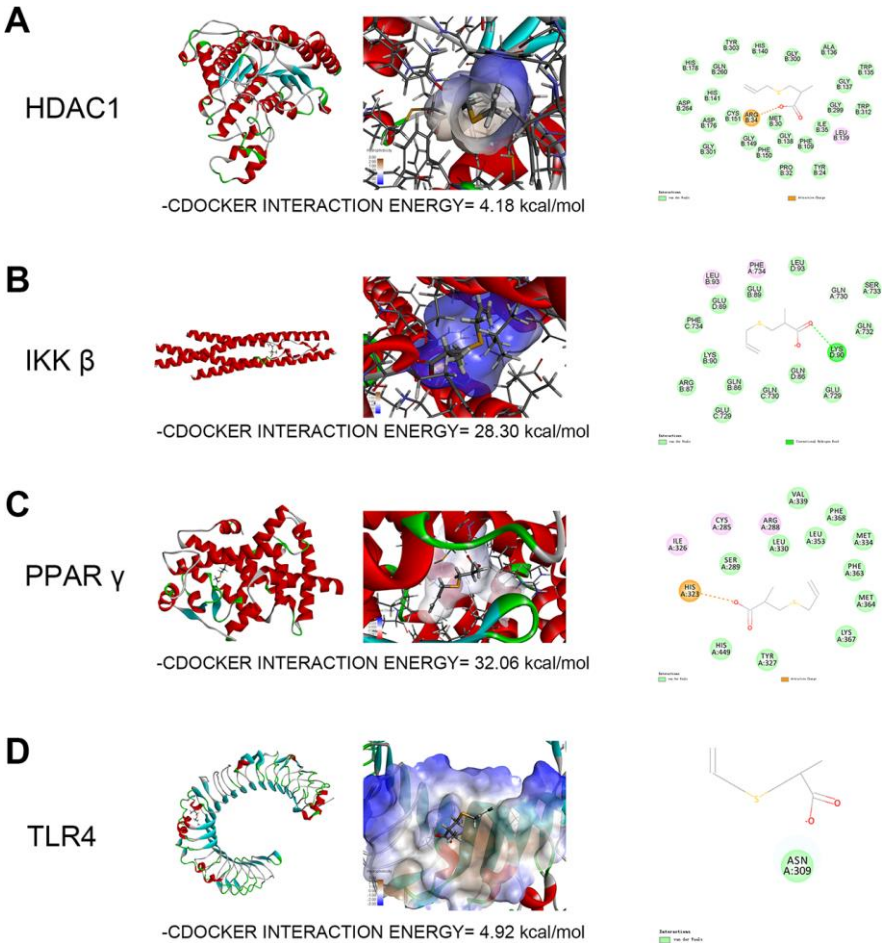

Supplementary Figure 1. Molecular docking analysis of SAC and its potential binding partners, HDAC1, IKKβ, PPARγ, and TLR4. (**A**) The 3D docking model shows -CDOCKER interaction energy value of 4.18 kcal/mol for the interactions between SAC and HDAC1 molecules. The 2D binding model between SAC and HDAC1 demonstrates 23 van der Waals interactions, 1 alkyl interaction, and 1 salt bridge between HDAC1 and SAC molecules. (**B**) The 3D docking model shows -CDOCKER interaction energy value of 28.3 kcal/mol for the interactions between SAC and IKKβ molecules. The 2D binding model between SAC and IKKβ demonstrates14 van der Waals interactions, 2 alkyl interactions, and 1carbon-hydrogen bond between IKKβ and SAC molecules. (**C**) The 3D docking model shows -CDOCKER interaction energy value of 32.06 kcal/mol for the interactions between SAC and PPARγ molecules. The 2D binding model between SAC and PPARγ demonstrates 11 van der Waals interactions, 3 alkyl interactions, and 1 salt bridge between SAC and PPARγ molecules. (**D**) The 3D docking model shows -CDOCKER interaction energy value of 4.92 kcal/mol for the interactions between SAC and TLR4 molecules. The 2D binding model between SAC and TLR4 demonstrates 1 van der Waal interaction between SAC and TLR4.

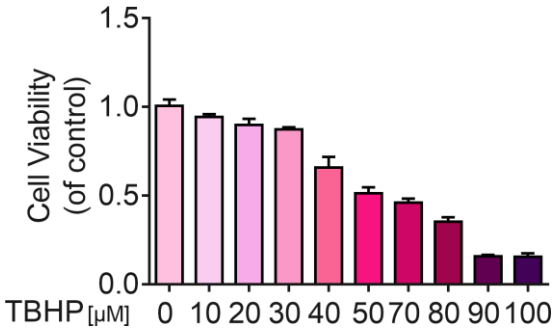

Supplementary Figure 2. CCK8 assay results show the viability of chondrocytes treated with different concentrations of TBHP for 2 h.